Open access • Journal Article • DOI:10.1029/94WR03038

Solving the Estimation-Identification Problem in Two-Phase Flow Modeling

Stefan Finsterle, Karsten Pruess

Published on: 01 Apr 1995 - Water Resources Research (John Wiley & Sons, Ltd)

Topics: Parameter identification problem, Inverse problem, Mathematical model, Sensitivity (control systems) and Estimation theory

Title
Solving the Estimation-Identification Problem in Two-Phase Flow Modeling

Journal
Water Resources Research, 31(4)

Authors
Finsterle, S.
Pruess, K.

Publication Date
1993-11-01

LBL-34853
UC-800
Preprint

Lawrence Berkeley Laboratory
UNIVERSITY OF CALIFORNIA

EARTH SCIENCES DIVISION

Submitted to Water Resources Research

Solving the Estimation-Identification Problem in Two-Phase Flow Modeling

S. Finsterle and K. Pruess

October 1993

Prepared for the U.S. Department of Energy under Contract Number DE-AC03-76SF00098

DISCLAIMER

LBL-34853
UC-800

Solving the Estimation-Identification Problem in Two-Phase Flow Modeling

Stefan Finsterle and Karsten Pruess

Earth Sciences Division
Lawrence Berkeley Laboratory
University of California
Berkeley, CA 94720

October 1993

This work was carried out under U.S. Department of Energy Contract No. DE-AC03-76SF00098 for the Director, Office of Civilian Radioactive Waste Management, Office of External Relations, and was administered by the Nevada Operations Office, U.S. Department of Energy, in cooperation with the Swiss National Cooperative for the Disposal of Radioactive Waste (Nagra).

Solving the Estimation-Identification Problem in Two-Phase Flow Modeling

STEFAN FINSTERLE[1] AND KARSTEN PRUESS

Earth Sciences Division, Lawrence Berkeley Laboratory

University of California, Berkeley, CA 94720

In this paper a procedure is presented to solve the estimation-identification problem in two-phase flow modeling. Given discrete observations made on the system response, an optimum parameter set is derived for an appropriate conceptual model by solving the inverse problem using standard optimization techniques. Subsequently, a detailed error analysis is performed, taking nonlinear effects into account. We discuss the iterative process of model identification and parameter estimation for a ventilation test performed at the Grimsel Rock Laboratory, Switzerland. A conceptual model is developed which allows accurate simulation of the evaporation of moisture at the drift surface and the induced propagation of the unsaturated zone into the formation. Two-phase flow parameters are estimated based on measurements of negative water potentials observed in granite rock near the ventilated drift. The error analysis reveals strong interdependencies among the parameters. These correlations can be reduced by appending additional information to the model, improving the overall quality of the estimation. The system behavior is discussed in detail for the optimum parameter set.

1. INTRODUCTION

Mathematical-numerical models commonly used to analyze or predict the response of groundwater systems have increasing capabilities for dealing with complex flow and transport processes. Simulation tools for non-isothermal flow of multiphase, multicomponent fluids have been developed for various applications to geothermal reservoir engineering, nuclear waste isolation studies, and unsaturated zone hydrology. However, greater model sophistication is usually accompanied by an increasing number of hydrogeologic parameters which enter the governing equations to describe the interaction between the fluids and the porous media. While some of the parameters affecting fluid flow in partially saturated formations can be directly obtained from laboratory experiments, such measured parameters may significantly differ from their model counterparts both conceptually and numerically mainly because of scale effects. In order to obtain model related formation parameters, the strategy is to calibrate the numerical model using observations of the system response at

---

[1] Previously at Laboratory of Hydraulics, Hydrology and Glaciology (VAW), Swiss Federal Institute of Technology (ETH), Zürich, Switzerland.

discrete points in space and time. The methodology of parameter estimation for saturated flow was reviewed by *Carrera and Neuman* [1986] and *Yeh* [1986]. Similar techniques have been applied to estimate parameters for unsaturated flow and transport processes [for a review see *Kool et al.*, 1987].

Three main aspects have to be considered when dealing with inverse modeling. The first and most important is referred to as model conceptualization. Model conceptualization can be defined as the process of approximating the relevant factors that control the behavior of the real flow system. It includes the specification of flow system geometry, formulation of constitutive relationships for multiphase flow, parametrization of the model domain, and the definition of appropriate initial and boundary conditions. While conceptualization is part of any modeling effort, it is important to realize that the parameters estimated by means of calibration procedures are only meaningful within the framework of the given conceptual model. Strictly speaking, they are model parameters rather than aquifer parameters. The second input to inverse modeling is the data. The type of quantities to be measured, the location of the observation points, and the duration of each measurement period have to be selected such that the parameters to be estimated are sensitive with respect to the data. Furthermore, most optimization procedures require some prior estimates of the measurement errors. The third aspect deals with the actual procedure of how to derive model parameters from the data observed in the field.

Modeling is an iterative process of developing model structures, for which an optimum parameter set is sought, followed by an interpretation of the remaining residuals which may point towards aspects of the model that need to be modified. Residual analysis for model identification requires a good deal of expertise and a sound understanding of the system behavior under two-phase flow conditions. Note, however, that the step of quantifying the parameters for a given model structure can be carried out based on rather objective mathematical criteria. On the other hand, model conceptualization involves more qualitative information and may be guided by the overall purpose of the modeling effort. We therefore first describe the procedure of solving the inverse problem to estimate parameters for a two-phase flow system. The modification of the underlying conceptual model will be discussed for a specific application.

The most widely employed approaches to solve the inverse problem minimize some norm of the differences between observed and model predicted state variables. If the view of maximum likelihood is taken, the performance criterion reflects the probability density

function of the final residuals. For normally distributed residuals correlated in space and time, it can be shown that maximizing the probability of reproducing the observed data leads to a method known as generalized nonlinear least squares estimation, for which a variety of optimization procedures have been developed [see e.g. *Scales*, 1985]. If the model is nonlinear in the parameters, minimization of the objective function is an iterative process in which information about the gradient and the convexity of the objective function is used to perform a downhill step toward the local minimum. One of the most generally applicable algorithms is the one proposed by *Levenberg* [1944] which was improved by *Marquardt* [1963]. The basic idea of the Levenberg-Marquardt method is to move along the steepest descent direction far from the minimum, and to switch continuously to the Gauss-Newton algorithm as the minimum is approached.

The strong nonlinearities inherent in two-phase flow make it difficult to minimize the objective function in an efficient and stable way. Reparametrization, such as logarithmic transformation of absolute permeabilities, and the incorporation of prior information about the parameters have been proposed to improve the properties of the objective function. Additionally, the robustness of the solution has to be questioned because the residuals almost never obey a Gaussian distribution. The assumption of normally distributed residuals, convenient because it leads to very powerful optimization procedures, may not be justified for two reasons. First, the errors associated with field data typically show much more outlier points than one would expect from the tail of the normal distribution. Secondly, a simulation model is only able to reproduce an average trend of the true system behavior due to the incompleteness and inaccuracy of the underlying conceptual model. As a result, the residuals, which contain both model and measurement errors, may have a substantial contribution from deviations which are systematic rather than random; consequently, they cannot be properly described by statistical measures. Nevertheless, least squares optimization has proved successful in many applications. Only a few alternative approaches have been proposed in the field of groundwater hydrology (for an example see the recent work by *Xiang et al.* [1993]).

The numerical model used to simulate non-isothermal two-phase flow is described in the next section. Subsequently, the standard least squares formulation and the minimization of the resulting objective function is summarized. The linearity assumption of the standard error analysis will be discussed in detail. Finally, the proposed method is applied to field data from an experiment performed at the Grimsel Rock Laboratory, Switzerland. Two-phase flow parameters are estimated based on measurements of negative water potentials observed in crystalline rock near a ventilated drift.

2. THE DIRECT PROBLEM

Given a conceptual model of the physical system and a set of values of the model parameters, the prediction of the system response for arbitrary initial and boundary conditions is referred to as the direct problem. In this work, the direct problem is solved with the two-phase two-component numerical simulator TOUGH2 [*Pruess*, 1987, 1991]. Consider a system with two mobile phases β (β=g: gas; β=l: liquid), and two components κ (κ=a: air; κ=w: water). The governing mass-balance equation for each component can be written in the following integral form [*Pruess and Narasimhan*, 1985]:

$$\frac{\partial}{\partial t}\int_V M^\kappa dv = \int_\Gamma \mathbf{F}^\kappa \cdot \mathbf{n}\, d\Gamma + \int_V q^\kappa dv \tag{1}$$

The integration here is over an arbitrary subdomain V of the flow system which is bounded by the closed surface Γ with inward normal vector $\mathbf{n}$. M^κ is the mass accumulation term for component κ, $\mathbf{F}^\kappa$ is the mass flux term, and q^κ is a term representing sinks and sources. The mass accumulation term is

$$M^\kappa = \phi \cdot \sum_{\beta=l,g} S_\beta \cdot \rho_\beta \cdot X_\beta^\kappa \tag{2}$$

where ϕ is porosity, S_β is phase saturation, ρ_β is density of phase β, and X_β^κ is the mass fraction of component κ in phase β. Thus, M^κ is the total mass of component κ present per unit volume.

The mass flux terms contain a sum over the two phases:

$$\mathbf{F}^\kappa = \sum_{\beta=l,g} \mathbf{F}_\beta \cdot X_\beta^\kappa \tag{3}$$

where the flux of phase β is:

$$\mathbf{F}_\beta = -k \cdot \frac{k_{r\beta}}{\mu_\beta} \cdot \rho_\beta \left(\nabla P_\beta - \rho_\beta \cdot \mathbf{g} \right) - \delta_{\beta g} \cdot D_{va} \cdot \rho_\beta \cdot \nabla X_\beta^\kappa \tag{4}$$

Here, k denotes absolute permeability, $k_{r\beta}$ is relative permeability of phase β as a function of saturation, μ_β is dynamic viscosity of phase β, P_β is the pressure in phase β, and **g** is gravitational acceleration. The last term in (4) contributes only to gas phase flow and represents an opposite diffusive flux for each of the components, with D_{va} the diffusion coefficient for vapor-air mixtures in porous media [*Vargaftik*, 1975; *Walker et al.*, 1981]:

$$D_{va} = \Omega^\kappa \cdot D_{va}^0 \frac{P_0}{P_g} \left(\frac{T}{T_0}\right)^\theta \tag{5}$$

where D_{va}^0 is the vapor diffusivity at standard conditions T_0 and P_0, and θ is a material parameter to account for temperature dependency. The parameter Ω^κ specifies properties relevant to binary diffusion in a porous medium. For air, it describes the restriction of the molecular diffusion to the gas filled fraction of the pore space, $\Omega^a = \tau \cdot \phi \cdot S_g$, where τ is a tortuosity factor. However, there is a great deal of evidence from studies in soil sciences for enhanced vapor diffusion from pore-level phase change processes [see e.g. *Walker et al.*, 1981]. The experimentally determined values $\Omega^w \approx 1$ for vapor diffusion are orders of magnitude larger than the parameter group $\tau \cdot \phi \cdot S_g$ for air diffusion. If no reliable measurements are available, ϖ^κ may be subjected to the estimation process.

Binary diffusion becomes an important factor for moisture transfer if large temperature gradients or strong capillary forces are present. The latter induce a decrease of the vapor partial pressure P_v according to Kelvin's equation:

$$P_v = P_{sat} \cdot \exp\left[\frac{P_c \cdot M_w}{\rho_l \cdot R \cdot T}\right] \tag{6}$$

where P_{sat} is saturated vapor pressure for a given absolute temperature T, $P_c = P_l - P_g$ is the capillary pressure, R is the universal gas constant, and M_w is the molecular weight of water. As a result, a capillary pressure gradient leads to a mass fraction gradient ∇X_g^κ which is the driving force for binary diffusion.

As part of the model conceptualization, a relatively simple parametric relationship has to be chosen to describe the two-phase hydraulic properties. *Luckner et al.* [1989] derived a consistent set of capillary pressure and relative permeability curves based on van Genuchten's model [*van Genuchten*, 1980]. The macroscopic capillary pressure P_c is a function of liquid saturation as follows:

$$P_c = -\frac{1}{\alpha}(S_e^{-1/m} - 1)^{1/n} \tag{7}$$

with the effective liquid saturation

$$S_e = \frac{S_l - S_{lr}}{1 - S_{lr}} \qquad (S_{lr} < S_l < 1) \tag{8}$$

where S_{lr} is the residual liquid saturation. The parameter α can be interpreted as the reciprocal of the air entry pressure, and parameter n reflects the pore size distribution of the porous medium. With m=1-1/n, and applying Mualem's predictive hydraulic conductivity model [*Mualem*, 1976], expressions for liquid and gas relative permeabilities can be derived:

$$k_{rl} = S_e^{\eta} \cdot \left[1 - (1 - S_e^{1/m})^m\right]^2 \tag{9a}$$

$$k_{rg} = (1 - S_e)^{\gamma} \cdot \left[1 - S_e^{1/m}\right]^{2m} \tag{9b}$$

where η and γ are pore connectivity parameters for the wetting and nonwetting phase, respectively.

The formulation of the direct problem must include appropriate equations of state. The thermophysical properties of liquid water and vapor are obtained from steam table equations [*International Formulation Committee*, 1967]. Air is treated as an ideal gas, and gas phase pressure is assumed to be the sum of air and vapor partial pressures. Air dissolution in liquid water is represented by Henry's law. The governing transport equations are discretized in space using an integral finite difference formulation [*Narasimhan and Witherspoon*, 1976]. Time is discretized fully implicitly as a first-order finite difference. Local thermodynamic equilibrium is assumed so that the conditions in each volume element (grid block) can be characterized by a set of thermodynamic state variables. Discretization results in a set of nonlinear coupled algebraic equations which are solved by means of Newton-Raphson iteration. A generalized minimum residual conjugate gradient solver is used to solve the linear equations arising at each iteration step [based on *Seager*, 1988].

3. THE INVERSE PROBLEM

3.1 Objective Function

The estimation of parameters for a given system model and a set of observed state variables is referred to as the inverse problem. The parameters to be determined are those which enter the numerical model that solves the direct problem. In the case of a drift ventilation experiment, these are the absolute permeability, the parameters of the capillary pressure and relative permeability functions, porosity and compressibility of the rock matrix, diffusion coefficient etc. Furthermore, initial and boundary conditions as well as geometrical features such as fracture spacing can be considered as unknown parameters. The parameters may refer to individual points, to elements of the discretized flow region, or to zones for which values are assumed constant. The objective of the inverse model is to provide improved estimates of these parameters by relying on certain measurements. Again, potential observation types are those for which a corresponding model output is calculated, e.g. gas pressure, water potential, gas and liquid flow rate, temperature and saturation measurements. Prior information about each of the parameters mentioned above can be added to the vector of observable variables. The indirect approach to inverse modeling consists of minimizing a performance criterion that measures the differences between observed and computed system response. The residual vector $\mathbf{r}$ summarizes the contributions from observations of different types i, i$\in$ {prior information, pressure, flow rate, saturation, ...}:

$$\mathbf{r}_i = \mathbf{y}_i^* - \mathbf{y}_i(\mathbf{p}) \tag{10}$$

Here, $\mathbf{y}_i^*$ is the vector of the observed state variables of type i, and $\mathbf{y}_i$ contains the corresponding model output which is a function of the unknown parameter vector $\mathbf{p}$. The number of elements in $\mathbf{r}_i$ is equal to the number of points in space and time at which data are available. The error structure of the residuals is assumed Gaussian and can therefore be described by a covariance matrix as follows:

$$\mathbf{C}_i = (\sigma_0^2)_i \cdot \mathbf{V}_i \tag{11}$$

The scalar σ_0^2 is termed prior error variance. It can be used to scale observations of different type against each other. With $\mathbf{V}_i$ being a positive definite matrix which represents the relative error structure, $\mathbf{C}_i$ reflects the expected uncertainty of the residuals of type i. If the quality of the data is not well known, one might consider estimating the statistical parameters along with the other model parameters. Provided that observations of different

types are uncorrelated, the objective function to be minimized can now be written as follows:

$$\zeta(\mathbf{p}) = \sum_i \left[\sigma_0^{-2} \cdot \mathbf{r}^T \mathbf{V}^{-1} \mathbf{r} \right]_i \tag{12}$$

Equation (12) is the sum of the squared residuals, weighted by the inverse of the prior covariance matrix. The index i denotes the type of the data being used for calibration, including prior information about the model parameters. The corresponding estimator is known as the generalized nonlinear least squares estimator. Based on maximum likelihood theory, it can be shown that minimizing ζ is equivalent to maximizing the probability of reproducing the observed system state, if the residuals follow a Gaussian distribution. Note that due to the normality assumption inherent in least squares, the corresponding estimator leads to biased parameters if large residuals occur more frequently than predicted by the normal distribution. In these cases, the objective function should be appropriately modified to improve the robustness of the estimator.

3.2 Minimization Algorithm

An appropriate algorithm is needed to minimize the objective function ζ. The least squares formulation suggests use of Newton-type minimization algorithms with quadratic convergence near the optimum. In Newton's method, the objective function ζ is locally approximated by a quadratic form which allows iterative computation of an improved parameter vector $\mathbf{p}_{new}$ from a previous estimate $\mathbf{p}_{old}$ as follows:

$$\mathbf{p}_{new} = \mathbf{p}_{old} - \mathbf{H}^{-1}(\mathbf{p}_{old}) \cdot \mathbf{g}(\mathbf{p}_{old}) \tag{13}$$

where $\mathbf{g}$ is a gradient vector, and $\mathbf{H}$ is the Hessian matrix. We mention in passing that (13) is a closed form solution for the unknown parameters if the model is linear. The Hessian matrix $\mathbf{H}$ is not only expensive to calculate, but may also become negative-definite if the model is strongly nonlinear. Levenberg has proposed a method to approximate the Hessian by a matrix $\mathbf{H}'$ that is easy to calculate and always positive-definite:

$$\mathbf{H}' = \mathbf{J}^T \mathbf{C}^{-1} \mathbf{J} + \mu \cdot \mathbf{D} \tag{14}$$

Here, $\mathbf{J}$ is the m×n Jacobian matrix with elements $J_{ij} = \frac{\partial r_i}{\partial p_j}$, where m is the total number of observations, and n is the number of parameters to be estimated. $\mathbf{D}$ denotes a diagonal matrix of order n with elements equivalent to the diagonal elements of matrix $\mathbf{J}^T \mathbf{C}^{-1} \mathbf{J}$. The scalar $\mu \geq 0$ is the so-called Levenberg parameter. If $\mu = 0$, (13) results in a Gauss-Newton step,

while a large value of μ represents a small step in the steepest descent direction. *Marquardt* [1963] has given a simple rule of how to continuously update the Levenberg parameter μ during the optimization procedure, switching from a gradient step far from the minimum to a Gauss-Newton step if the minimum is approached. The reason for choosing the Levenberg-Marquardt algorithm to minimize the objective function is its robustness far from the optimum, where the topology of the objective function may be complicated due to the nature of the two-phase flow formulation. Furthermore, when approaching the optimum, nonlinear effects are somewhat reduced which allows use of Gauss-Newton steps near the minimum.

3.3 Error analysis

An uncertainty measure of the estimated parameter values is usually obtained under the assumption of normality and linearity. The normality assumption is based on the fact that the distribution of a sum of random values always tends to normal if the sample size is sufficiently large. The linearity assumption postulates that the model output can be approximated by a linear function of the parameters within the area covered by the confidence region. Both assumptions have to be questioned for parameter estimation in groundwater hydrology because the sample size is usually small and the two-phase flow model is highly nonlinear. In this section, we first derive the covariance matrix for the linear case. We then discuss a procedure originally proposed by *Carrera* [1984] to better approximate the true confidence region in the nonlinear case.

The $100(1-\alpha)\%$ confidence region for the true but unknown parameter vector $\bar{\mathbf{p}}$ contains those values $\mathbf{p}$ for which [*Donaldson and Schnabel*, 1987]

$$\zeta(\mathbf{p}) - \zeta(\hat{\mathbf{p}}) \leq s_0^2 \cdot n \cdot F_{n,m-n,1-\alpha} \tag{15}$$

where $\hat{\mathbf{p}}$ is the vector holding the optimum parameter set, s_0^2 is the estimated residual variance, and $F_{n,m-n,1-\alpha}$ is a quantile of the F-distribution. Here, α is the probability to reject the hypotheses even though it was true. In the general case, this confidence region is of arbitrary shape bounded by the points of constant likelihood. Its construction requires solving the direct problem many times in order to produce the corresponding contour of the objective function. Linearization methods have the advantage that their resulting confidence region is ellipsoidal, making it inexpensive to construct and easy to report. For a maximum likelihood estimator, the variance-covariance matrix is asymptotically given by

$$\hat{\mathbf{C}} = s_0^2\, \mathbf{H}(\hat{\mathbf{p}})^{-1} \tag{16}$$

where ^ indicates, that the quantity is an a posteriori estimate of the corresponding variable. By linearizing the model $\mathbf{y}(\mathbf{p})$ by the affine approximation around $\hat{\mathbf{p}}$

$$\mathbf{y}(\mathbf{p}) \approx \mathbf{y}(\hat{\mathbf{p}}) + \mathbf{J}(\hat{\mathbf{p}})\cdot(\mathbf{p} - \hat{\mathbf{p}}) \tag{17}$$

we obtain for the covariance matrix of the estimated parameter set the following expression:

$$\hat{\mathbf{C}} = s_0^2\cdot(\mathbf{J}^T\, \mathbf{V}^{-1}\, \mathbf{J})^{-1} \tag{18}$$

with

$$s_0^2 = \frac{\mathbf{r}^T\, \mathbf{V}^{-1}\, \mathbf{r}}{m - n} \tag{19}$$

Since the estimated error variance s_0^2 is a random variable, it can be tested against the prior error variance σ_0^2. If the deviation between the two values is statistically significant, then the conceptual model provides an unlikely match to the data. Consequently, the estimated parameter set has to be questioned as well. However, a failure of the model test may also indicate that the assumption about the error structure of the residuals was too optimistic.

We can now construct the confidence region for the linearized case consisting of those values $\mathbf{p}$ for which

$$(\mathbf{p} - \hat{\mathbf{p}})^T\, \hat{\mathbf{C}}^{-1}\, (\mathbf{p} - \hat{\mathbf{p}}) \le n\cdot F_{n,m-n,1-\alpha} \tag{20}$$

The confidence region given by (20) is a succinct representation of the region defined by (15). Recall that the covariance matrix $\hat{\mathbf{C}}$ approximates the actual surface of the objective function at its minimum by a tangent hyperellipsoid under the assumption of normality and linearity. If the model is nonlinear, the coverage of the confidence region by the linear approximation may be very poor with respect to both its size and its shape. Reparametrization is a possibility to reduce nonlinearity effects and the asymmetry of the confidence region.

Let us now assume that the shape of the confidence region is close to ellipsoidal, and that the orientation of the hyperellipsoid in the n-dimensional parameter space is accurately obtained from the linear error analysis. Then, by only adjusting the average size of the hyperellipsoid, we can better approximate the confidence region without losing the advantage of producing easily understandable results which are also simple to report. *Carrera* [1984] proposed a correction for the covariance matrix to account for nonlinearity. We adapt his

basic idea of comparing the actual likelihood function with the results from the linear approximation at discrete points in the parameter space. These test points are preferably located along the axis of the hyperellipsoid:

$$\tilde{\mathbf{p}}_{i\pm} = \hat{\mathbf{p}} \pm \sqrt{n \cdot F_{n,m-n,1-\alpha}} \cdot a_i \cdot \mathbf{u}_i \qquad (i=1..n) \qquad (21)$$

Here, $\tilde{\mathbf{p}}_{i\pm}$ are two test parameter sets on the i-th axis, the direction of which is given by the eigenvector $\mathbf{u}_i$ of the covariance matrix $\hat{\mathbf{C}}$. Note that the distance from the optimal parameter set $\hat{\mathbf{p}}$ is selected as a multiple of the corresponding eigenvalue a_i^2 and the quantile of the F-distribution. This means that the correction is tailored to approximate the confidence region on a certain confidence level $1-\alpha$. The eigenvalues a_i^2 which represent the length of the semiaxis are now corrected as follows:

$$a'^2_i = a_i^2 \cdot s_0^2 \cdot \left(\frac{A_+ + A_-}{2} \right)_i \qquad (22)$$

with

$$A_{\pm i} = \frac{n \cdot F_{n,m-n,1-\alpha}}{\zeta(\tilde{\mathbf{p}}_{i\pm}) - \zeta(\hat{\mathbf{p}})} \qquad (23)$$

Finally, the new covariance matrix is back-calculated from the eigenvectors $\mathbf{u}_i$ and the updated eigenvalues a'^2_i. The proposed correction requires 2n additional solutions of the direct problem and is thus relatively inexpensive. While the resulting confidence region is ellipsoidal by definition, the differences between $\zeta(\tilde{\mathbf{p}}_+)$ and $\zeta(\tilde{\mathbf{p}}_-)$ provide, as a byproduct of the correction procedure, some insight into the asymmetry of the true confidence region.

4. APPLICATION TO FIELD DATA

4.1 Introduction and Problem Description

The inverse modeling formulation outlined in the previous section has been implemented in a computer program named ITOUGH2 [*Finsterle*, 1993b] which has been verified by applying the code to synthetic test cases [*Finsterle*, 1993a]. The purpose of this section is to illustrate the applicability of the proposed methodology to field data that reveal strong two-phase flow effects.

A series of ventilation tests has been conducted at the Grimsel Rock Laboratory, Switzerland, a research facility operated by Nagra, the Swiss National Cooperative for the Disposal of Radioactive Waste. Ventilation tests were originally conceived to determine the macro-permeability of crystalline rocks by measuring the total inflow into drift sections with controlled ventilation. In these tests, ventilation is simply viewed as a convenient means to convey the incoming moisture to a measuring device [*Kull et al.*, 1991]. Accordingly, the standard interpretation of these tests is based on assuming that flow toward the drift is single-phase liquid. However, the estimated matrix permeabilities may be affected by partial drying of the drift wall leading to substantial regions with two-phase flow conditions. In order to quantify the extent of the two-phase region and study its hydraulic properties, a joint project between the Institute of Terrestrial Ecology, ETH Zürich, and Nagra has been initiated. In-situ measurements of water potential, water content, temperature, and ambient air humidity were performed during a ventilation test starting November 26, 1991, reported in *Gimmi et al.* [1992].

The ventilation experiment is conceptualized as follows (see Figure 1). We expect the flow regime to be radial in the vicinity of the drift. The computational region extends from the drift wall of radius 1.75 m to a presumably unaffected outer boundary at a distance of 6.75 m. A constant pressure of 0.37 MPa is prescribed at the outer boundary, reflecting the undisturbed pressure at drift level. Gravity effects are neglected. The flow region is partitioned into 200 grid blocks with logarithmically increasing radial distances. The experimental site is located in mildly deformed granodiorite that is considered homogeneous on the scale of interest. Two boreholes (BOVE 84.011 and BOVE 84.018) were drilled parallel to the drift. They are equipped with conventional pressure transducers to observe the hydraulic head. Thermocouple psychrometers (TP) were installed at six different depths (2, 5, 10, 20, 40, and 80 cm from the drift wall). They measure negative water potentials in the partially saturated region as a function of time. An estimate of the total inflow to large, sealed

off sections of the drift is obtained from measurements of the moisture extracted from the circulated air in a cooling trap. On a much smaller scale, the evaporation rate at the drift surface is estimated by measuring gradients of relative humidity and temperature.

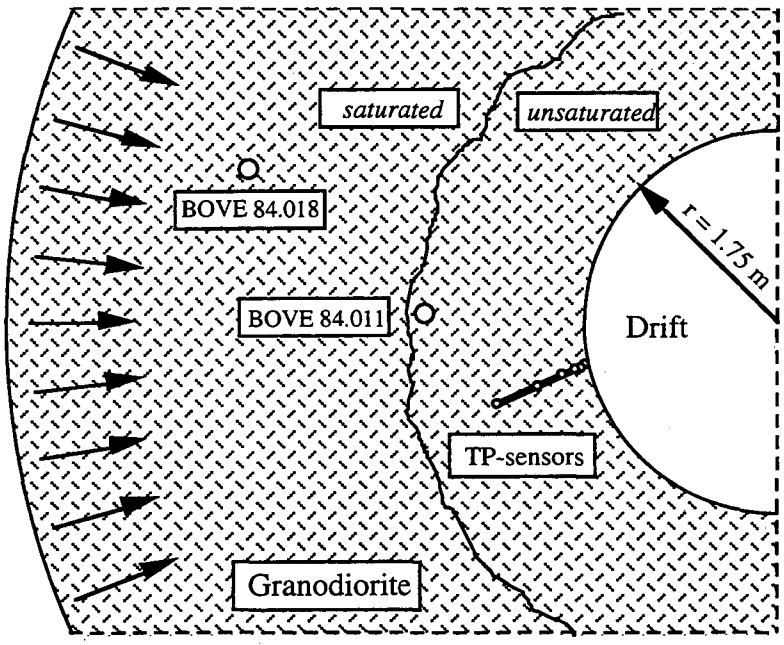

Figure 1: Schematic of model domain

4.2 Simulation Results

In this section, we discuss the formulation of the direct problem and the results of the forward calculation using the optimum parameter set. Prior to ventilation, the system is run to steady-state in order to obtain the initial pressure and saturation distribution and to evaluate the inflow to the drift under single-phase flow conditions. However, by reducing the pressure in the drift, air which is dissolved in the liquid phase from previous ventilation experiments comes out of solution, leading to a very small initial gas saturation throughout the model domain. Starting ventilation, formation water evaporates at the surface due to the reduced relative humidity which is the main physical process that drives the desaturation of the formation. *Connell and Bell* [1993] show that the transfer of moisture at a free surface is a complicated mechanism which depends on factors such as relative humidity, temperature gradient, wind velocity in the drift, and surface roughness, the latter two defining the thickness of the laminar boundary layer and the magnitude of the effective vapor diffusion coefficient in the drift. Rather than explicitly model the moisture transfer across the drift surface, the reduced relative humidity is imposed as a boundary condition at the drift wall,

giving rise to an equivalent capillary suction according to Kelvin's equation [*Edlefsen and Anderson*, 1943]:

$$P_{c,equ} = \ln (h)\, \rho_l \cdot \frac{R \cdot T}{M_w} \tag{24}$$

The relative humidity h in the drift is 68% at a temperature of 12.5 °C during the first 10 days of the experiment, 71% at T=13.0 °C for the next 50 days, and 75% during the remaining 20 days, invoking an equivalent capillary suction of -50.0, -46.0, and -38.0 MPa, respectively. By prescribing these values directly at the drift wall, we neglect the variation of the vapor content in the boundary layer as a function of wind velocity and the actual evaporation rate. A sensitivity study was performed to assess the robustness of this model conceptualization. It turned out that the system behavior is relatively insensitive with respect to the boundary suction pressure and the strength of the vapor diffusion at the drift wall. This is mainly due to the fact that the evaporation rate is limited by the water supply from the formation which is governed by the two-phase characteristics of the rock. Increased evaporation at the surface immediately leads to higher gas saturations at the drift wall which reduces the liquid relative permeability, thus limiting the water supply for evaporation. On the other hand, vapor diffusion toward the drift is increased because of vapor pressure lowering effects which lead to larger concentration gradients for binary diffusion. However, the contribution of vapor diffusion to the total mass flow of water is small, except at the surface itself. The finding that the water inflow to the drift is relatively stable is also confirmed by the results of discrete evaporation measurements near the drift wall [*Vomvoris and Frieg*, 1991]. This data shows that the temporal variations of evaporation rates due to changing climate conditions in the drift are very minor compared to the dramatic change of the equivalent suction pressure that has been applied in that experiment.

Figure 2 shows the calculated flow rate into the drift as a function of time. It can be seen that the flow rate does not seem to be affected by the changes in the relative humidity and associated capillary pressure at the drift wall. The average flow rate of water over 80 days in both liquid and vapor phase is 0.34 $mg \cdot m^{-2} \cdot s^{-1}$ which is larger than the steady-state inflow under single-phase liquid conditions. Obviously, there is an increase of the amount of moisture that is removed from the formation due to evaporation. However, since the flow regime is radial and finite, the system tends towards equilibrium between the evaporation rate at the drift surface and the incoming liquid from the formation so that the expansion of the unsaturated zone slows down over time. The net loss of liquid in the model region is compensated by a counterflow of gas from the drift into the rock.

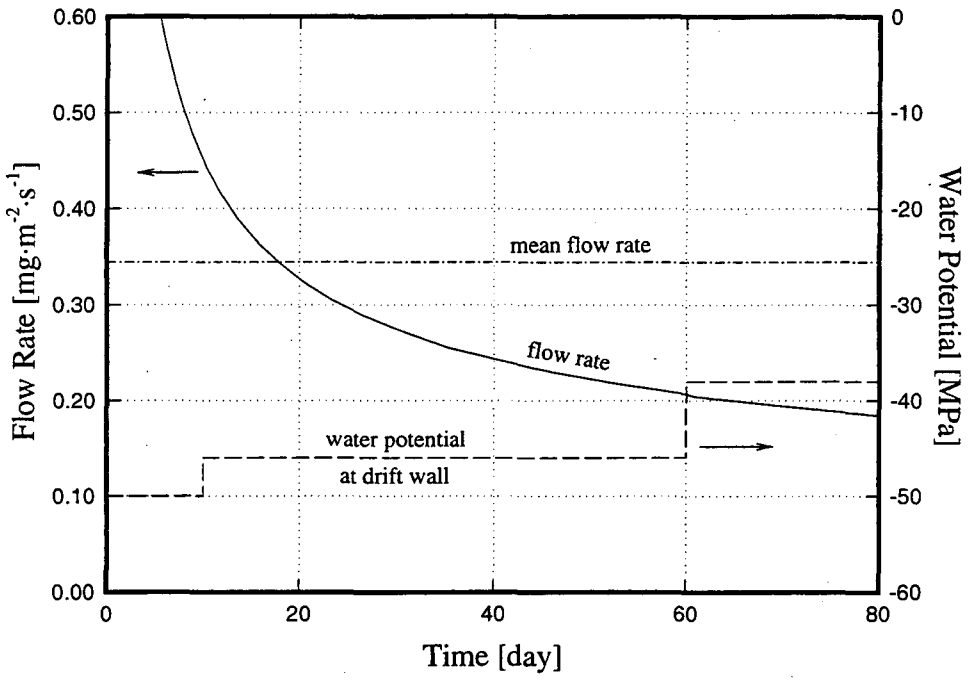

Figure 2: Flow rates and suction pressure at the drift wall as a function of time

Figure 3 depicts the pressure profile prior to ventilation, and the final distribution after 80 days. The gas pressure throughout the partially saturated zone is close to atmospheric. It does, however, remain slightly above the fixed pressure in the drift, mediated by diffusive flow of air and vapor across the drift wall. The presence of a low pressure region - with respect to the profile from single-phase liquid flow - has been observed in the two parallel boreholes BOVE 84.011 and BOVE 84.018, leading to speculation about the impact of the unsaturated zone on head and inflow measurements [*Vomvoris and Frieg*, 1992]. The computed gas pressure at the location of the two boreholes is 0.148 and 0.296 MPa which compares reasonably well with the observed value of 0.12 and 0.28 MPa, respectively. Note that the formation is partially desaturated by evaporation to a depth of about 1.5 m. However, significant gas saturations (e.g. > 50 %) are found only to a depth of a few centimeters from the surface. The shape of the saturation profile strongly depends on the parametric model that describes the capillary pressure as a function of liquid saturation.

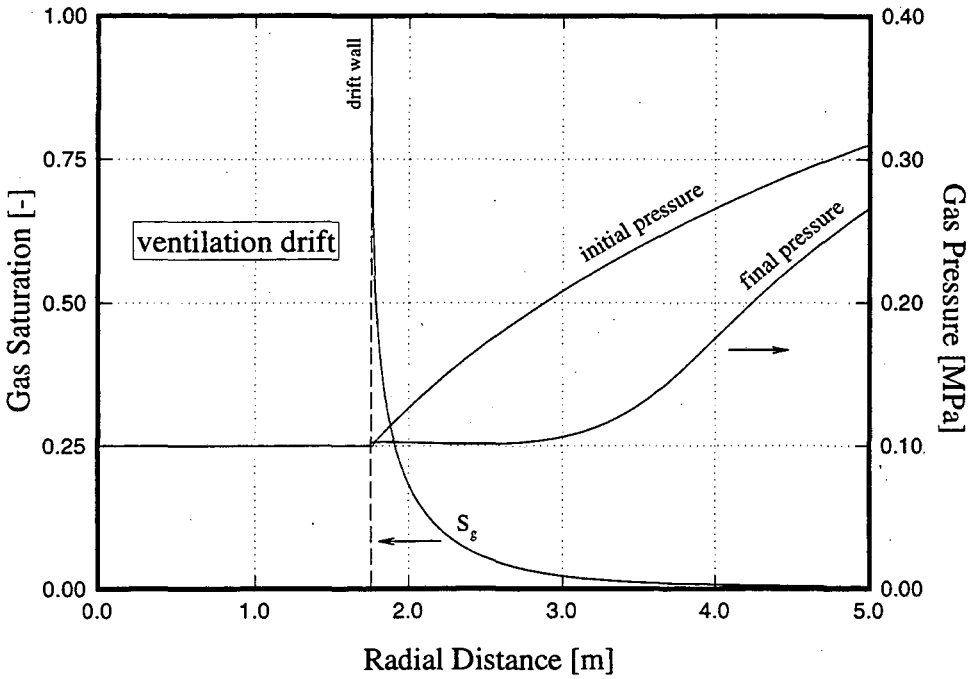

Figure 3: Gas saturation and pressure profiles

4.3 Inverse Modeling Results

For the conceptual model described above, and based on the water potentials measured at 25 logarithmically spaced points in time during a ventilation period of 80 days, we estimate three parameters, namely the absolute permeability k, and the parameters n and $1/\alpha$ of van Genuchten's characteristic curves described by Eqs. (7) and (9). Besides developing a flow simulation model, inverse modeling requires assigning prior variances to the residuals reflecting both errors from the measurements and errors from the model conceptualization. We assume that the standard deviation of each residual is 10 % of the measured value, and that the residuals are uncorrelated. Furthermore, we employ a reparametrization for absolute permeability and estimate its logarithm instead of the value itself. An initial guess is provided for each of the unknown parameters, and the ITOUGH2 code is run applying least squares optimization. Figure 4 shows observed and computed water potentials for the calibrated model.

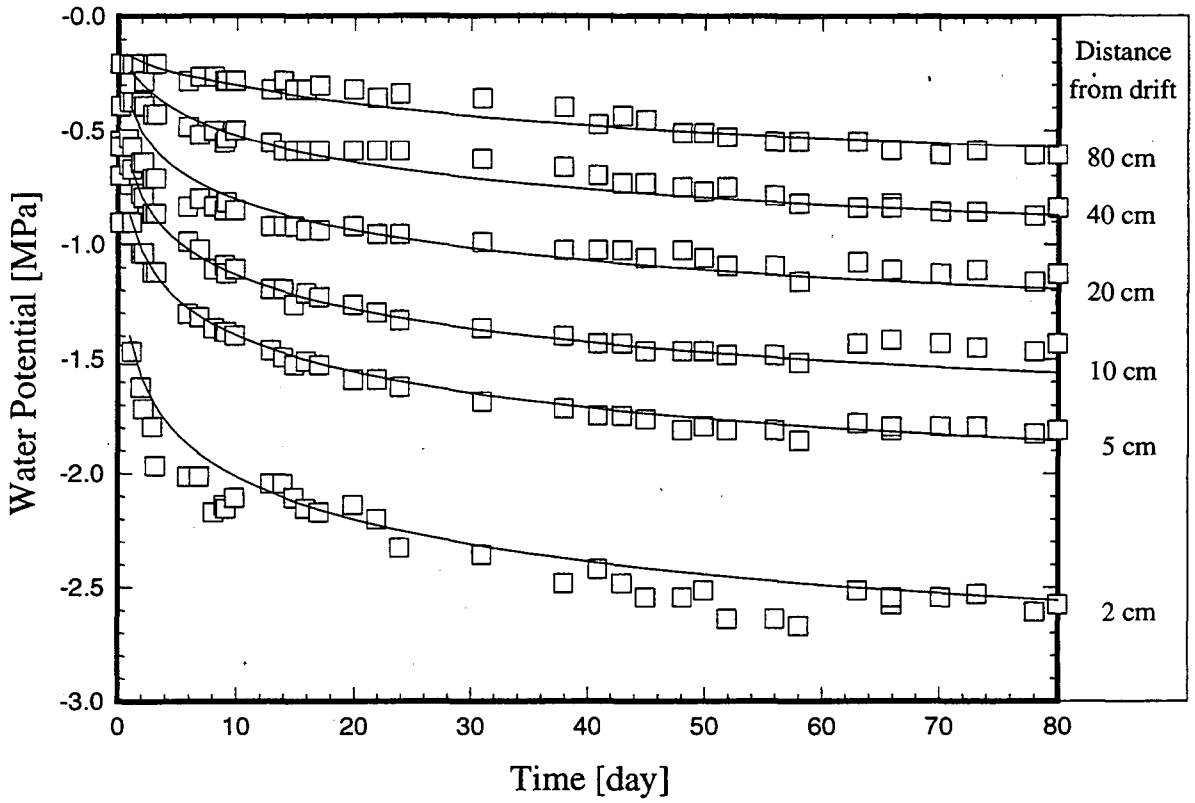

Figure 4: Fit between computed (lines) and measured (symbols) water potentials

First, we note that our model is capable of reproducing the overall behavior of the two-phase flow system. Both the magnitude and the trend of the capillary pressures are well reproduced by the model results. This visual finding is confirmed by the estimated residual variance, $s_0^2 = 1.07$, which indicates that the achieved match is consistent with our expectations regarding the final residuals. The results are summarized in Table 1 (estimated parameter set, eigenvalues and eigenvectors of covariance matrix) and Table 2 (covariance and correlation matrices). Identical results were obtained starting the minimization procedure from different points in the parameter space, ranging from -17.0 to -21.0 for log(k), 10.0 to 20.0 bar for $1/\alpha$, and 1.0 to 3.0 for n. This indicates that the inverse problem is well-posed and that the solution is unique.

Parameter	Estimate	Eigenvalue	Eigenvector		
log (k)	-18.29	2.10×10^{-4}	0.851	0.512	0.115
n	2.38	1.68×10^{-3}	-0.495	0.856	-0.147
$1/\alpha$ [bar]	15.77	1.41×10^{-1}	-0.173	0.068	0.982

Table 1: Parameter estimates, eigenvalues and eigenvectors of estimation covariance matrix

	log (k)	n	$1/\alpha$
log (k)	4.81×10^{-3}	-0.75	-0.93
n	-2.28×10^{-3}	1.94×10^{-3}	0.57
$1/\alpha$	-2.39×10^{-2}	9.23×10^{-3}	1.36×10^{-1}

Table 2: Covariance (diagonal and lower triangle) and correlation (upper triangle) matrices

The correlation matrix reveals strong interdependencies between all parameters. Since decreasing the value for n reduces the liquid relative permeability, the absolute permeability has to be increased in order to maintain a certain water flow rate. This explains why n and log(k) are negatively correlated. Similarly, the water potentials decrease with higher air entry pressure and higher permeability, leading to a negative correlation between these two parameters. The correlation between n and $1/\alpha$ is difficult to predict because the effect of these parameters on capillarity changes with saturation. Since the propagation of the unsaturated front depends on absolute permeability, thus determining the saturation at each of the tensiometers, the correlation between the two van Genuchten parameters is indirectly affected by their correlations with log(k). The parameter $1/\alpha$ is almost entirely associated with the largest eigenvalue, indicating a relatively uncertain estimate. Parameter combinations along the corresponding eigenvector are therefore most unreliable. Furthermore, the eigenvector associated with log(k) shows relatively large components in the two other parameters.

From this correlation structure it can be concluded that determining the absolute permeability by means of independent data may greatly reduce the correlations among all three parameters and therefore improve the quality of the estimation. In order to do this, we select the total inflow rate of moisture to the drift as an additional data point, expecting that it

is a very sensitive measure with respect to changes of the absolute permeability. However, inflow measurements from larger drift sections contain significant contributions from highly conductive shear zones, which would lead to systematic errors. By covering these shear zones with plastic sheeting, the mean flow rate of water extracted from the granodiorite matrix is estimated to be in the order of 0.3×10^{-6} kg·s^{-1}·m^{-2} [*Kull et al.*, 1991]. This is consistent with small scale measurements of evaporation rates at the drift wall, where values between 0.4×10^{-6} and 1.3×10^{-6} kg·s^{-1}·m^{-2} were observed during a short-term ventilation experiment with a relative humidity of 65 % [*Vomvoris and Frieg*, 1991]. These values are higher than the average rate because they are taken at the beginning of a climatic change where increased inflow is expected (see Figure 2).

For our inverse modeling study, we calculate the total inflow to the drift as a TOUGH2 - model result and compare it to the measured value given by *Kull et al.* [1991]. Even though relatively uncertain, a low standard deviation of 10^{-8} kg·s^{-1}·m^{-2} is assigned to this additional data point, accounting for the fact that it represents a mean value which has to be appropriately weighted against the $6\times25 = 150$ individual water potential measurements. Furthermore, we include two gas pressure measurements in our model, taken at boreholes BOVE 84.011 and BOVE 84.018 (see Figure 1). The extent of the reduced pressure zone as shown in Figure 3 is reflected in these data. A pressure of 0.12 MPa and 0.28 MPa, respectively, is observed in the corresponding intervals. They are compared with the computed pressure at the end of the modeled ventilation period. A standard deviation of 0.01 MPa is assigned. Finally, we take the estimates of the previous run as prior information about the parameters. They are weighted by the inverse of the variances given in Table 2.

The results of the inverse run using the extended data set are summarized in Tables 3 and 4. First we note that taking into account the flow and gas pressure measurements results in a slightly lower value for the absolute permeability. The other two parameters are shifted according to the correlation rules discussed above. The resulting characteristic curves are shown in Figure 5. The variances of all estimates have been reduced due to the fact that more independent information is involved in the determination of the parameter values. The reduction of the variances is stronger than those of the eigenvalues, indicating that the improvement is also caused by weakening the correlations among the parameters, as is shown by the covariance matrix. Predicted water potentials are virtually indistinguishable from the previous calculation as plotted in Figure 4, because the parameter set has been shifted basically along the eigenvector associated with the largest scaled eigenvalue.

Parameter	Estimate	Eigenvalue	Eigenvector		
log (k)	-18.51	1.42×10^{-4}	0.921	0.377	0.095
n	2.46	1.09×10^{-3}	-0.377	0.926	-0.022
$1/\alpha$ [bar]	17.04	3.05×10^{-2}	-0.097	-0.015	0.995

Table 3: Parameter estimates, eigenvalues and eigenvectors of estimation covariance matrix

	log (k)	n	$1/\alpha$
log (k)	5.61×10^{-4}	-0.39	-0.71
n	-2.86×10^{-4}	9.61×10^{-4}	-0.09
$1/\alpha$	-2.92×10^{-3}	-4.85×10^{-4}	3.03×10^{-2}

Table 4: Covariance (diagonal and lower triangle) and correlation (upper triangle) matrices

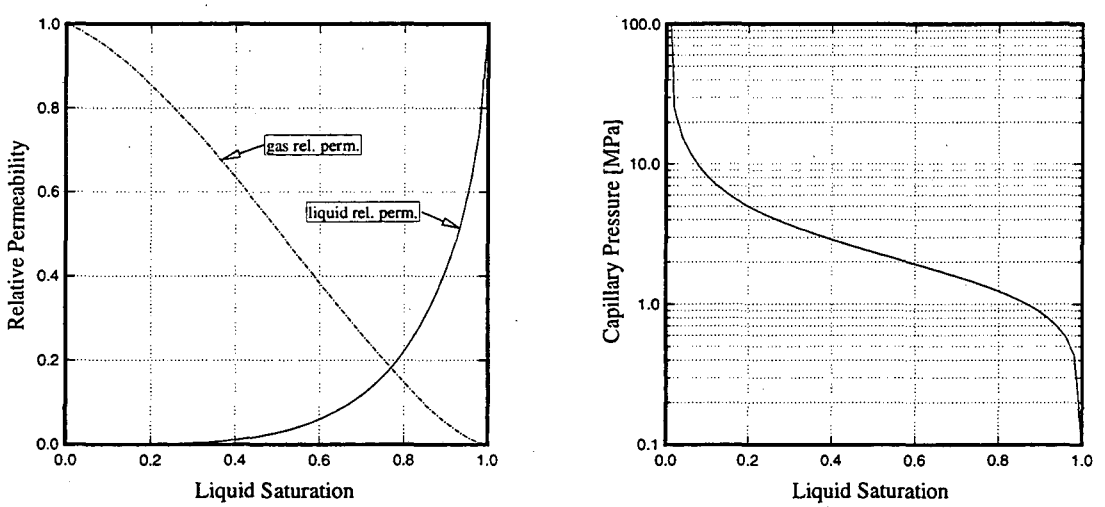

Figure 5: Characteristic curves estimated by inverse modeling

In the remainder of this paper we will show that the actual confidence region around the optimum parameter set can be accurately represented by a covariance matrix that is corrected to account for nonlinearities. The procedure is demonstrated for the two parameters n and $1/\alpha$ of van Genuchten's characteristic curves whereas the absolute permeability is fixed at its optimum value. By evaluating the objective function for many parameter combinations, a contour map can be drawn (Figure 6), depicting the location and convexity of the minimum.

From Equation (15) we see that the actual confidence region on a given significance level

α is bounded by the contour of the objective function on level $\zeta(\hat{\mathbf{p}}) + s_0^2 \cdot n \cdot F_{n,m-n,1-\alpha}$. For two parameters and 155 data points, the quantile of the F-distribution on the 95%-confidence level is $F_{2,153,0.95} = 3.054$. The linear approximation of this confidence region is given by (20). We then increase the corresponding eigenvalues following the procedure outlined in Section 3.3. As a result, the actual confidence region is accurately represented by an ellipse the orientation of which is calculated from the standard linear error analysis, and its size is appropriately corrected to account for nonlinearities. The increase of the eigenvalues which is necessary to better approximate the actual confidence region shows that linear error analysis provides too optimistic a measure of the estimation error. This is due to the fact that (20) intrinsically describes a minimum variance bound. Furthermore, it is shown that the shape of the actual confidence region is close to ellipsoidal so that its description by means of a covariance matrix seems justified in this case. Finally, the approximation of the Hessian by the matrix $\mathbf{J}^T \mathbf{V}^{-1} \mathbf{J}$ is accurate enough to obtain the orientation of the confidence region, i.e. the eigenvectors of the corresponding covariance matrix (18). This concludes the discussion of the nonlinear error analysis.

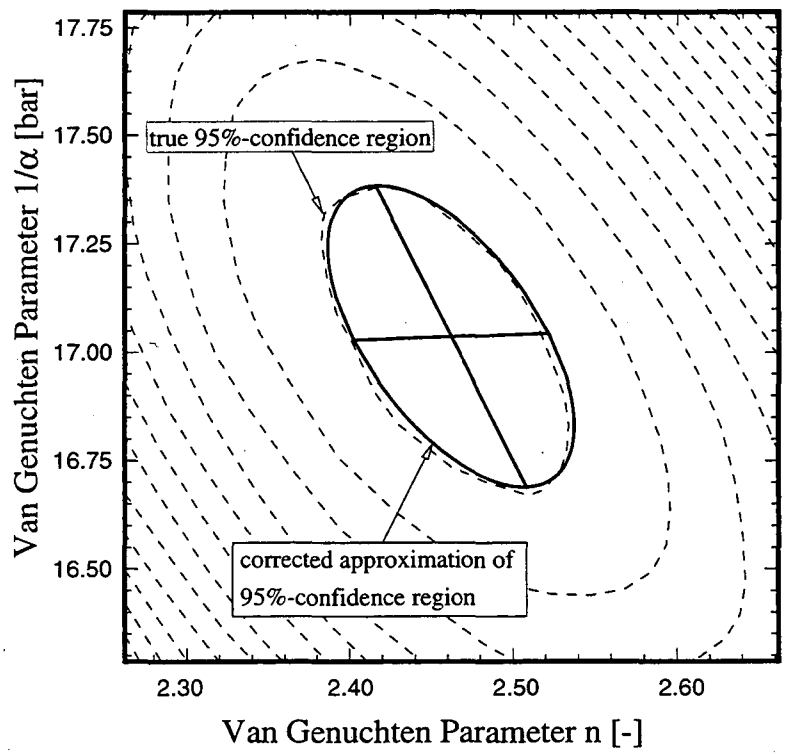

Figure 6: Contours of objective function, true confidence region, and corrected confidence region from linear approximation

5. CONCLUDING REMARKS

Three major aspects of inverse modeling in groundwater hydrology have been addressed in this paper:

1. The problem of parameter estimation is solved for the simulation of groundwater systems that contain two immiscible phases. While the direct measurement of two-phase parameters is both conceptually difficult and experimentally expensive, inverse modeling provides an appealing technique to obtain model-related parameters by calibrating the numerical model against sensitive observations of the system state.

2. The inverse problem is formulated in the framework of maximum likelihood estimation theory. The objective function from generalized least squares optimization is minimized using the Levenberg-Marquardt algorithm. The efficiency of the procedure allows examination of different model structures and different data sets, improving the understanding of the two-phase flow system. Furthermore, the analysis of sensitivity coefficients and the correlation structure provides some guidance for the design of future experiments.

3. One of the main advantages of inverse modeling is that the quality of the estimation can be described by statistical measures. However, if the model is highly nonlinear, the standard linear error analysis overestimates the accuracy of the optimum parameter set. Based on an idea originally presented by *Carrera* [1984], we calculate a corrected covariance matrix which approximates the true confidence region in the nonlinear case. The procedure is computationally inexpensive and leads to easily reportable confidence regions.

The method of parameter estimation by inverse modeling has been applied to data from a ventilation test performed at the Grimsel Rock Laboratory. The following major conclusions can be drawn from this field application:

1. We successfully modeled a field experiment conducted under two-phase flow conditions. The conceptual model incorporates a variety of physical processes, including evaporation at the drift surface, capillary forces and phase interferences, and binary diffusion of water vapor and air driven by vapor pressure lowering effects. A sensitivity analysis has been

performed to assess the main features of the conceptual model. Since the system response is sensitive with respect to the input parameters of the numerical model, observations of different types can be used to determine the properties of interest.

2. Inverse modeling of the ventilation experiment provides reliable estimates of model-related formation parameters affecting two-phase flow. If the absolute permeability can be determined independently, the parameters of van Genuchten's characteristic curves are estimated with less uncertainty because the indirect correlation to the absolute permeability is reduced.

3. If the model is strongly nonlinear in the parameters, the standard way of calculating error bounds on the parameters leads to too optimistic variances. The nonlinear error analysis proposed in this paper provides an improved estimate of the confidence region.

Acknowledgments. This work was carried out under U.S. Department of Energy Contract No. DE-AC03-76SF00098, for the Director, Office of Civilian Radioactive Waste Management, Office of External Relations, and was administered by the Nevada Operations Office, U.S. Department of Energy, in cooperation with the Swiss National Cooperative for the Disposal of Radioactive Waste (Nagra). Much of this paper is based on research performed at the Laboratory of Hydraulics, Hydrology and Glaciology (VAW), ETH Zürich, in collaboration with Nagra. We are especially greatful to J. Trösch and U. Kuhlmann (VAW), and S. Vomvoris (Nagra) for their support. We would also like to thank T. Gimmi, Institute of Terrestrial Ecology, ETH Zürich, for providing most of the input data for the field example. We thank C. Doughty, G. Moridis and J. Najita, Lawrence Berkeley Laboratory, for their careful reviews.

REFERENCES

Carrera, J., Estimation of aquifer parameters under transient and steady state conditions, Ph.D. Dissertation, Dep. of Hydrol. and Water Resour., Univ. of Arizona, Tucson, 1984.

Carrera, J., and S. P. Neuman, Estimation of aquifer parameters under transient and steady state conditions: 1. Maximum likelihood method incorporating prior information, *Water Resour. Res.*, 22(2), 199-210, 1986.

Connell, L. D., P. R. F. Bell, Modeling moisture movement in revegetating waste heaps, 1. Development of a finite element model for liquid and vapor transport, *Water Resour. Res.*, 29(5), 1435-1443, 1993.

Donaldson, J. R., and R. B. Schnabel, Computational experience with confidence regions and confidence intervals for nonlinear least squares, *Technometrics*, 29(1), 67-82, 1987.

Edlefsen, N. E. and A. B. C. Anderson, Thermodynamics of soil moisture, Hilgardia, 15(2), 31-298, 1943.

Finsterle, S., Inverse Modellierung zur Bestimmung hydrogeologischer Parameter eines Zweiphasensystems, Mitteilung Nr. 121 der Versuchsanstalt für Wasserbau, Hydrologie und Glaziologie an der ETH Zürich, Switzerland, 1993a.

Finsterle, S., ITOUGH2 User's Guide, Report No. LBL-34581, Lawrence Berkeley Laboratory, Berkeley, CA , 1993b.

Gimmi, T., H. Wydler, T. Baer, H. Abplanalp, H. Flühler, Near field desaturation experiment at the Grimsel Test Site (FLG), Nagra Internal Report, Wettingen, Switzerland, 1992.

International Formulation Committee, A formulation of thermodynamic properties of ordinary water substance, IFC Secretariat, Düsseldorf, Germany, 1967.

Kool, J. B., J. C. Parker, and M. T. van Genuchten, Parameter estimation for unsaturated flow and transport models - a review, *Journal of Hydrol.* 91, 255-293, 1987.

Kull, H., W. Brewitz, and K. Klarr, Felslabor Grimsel: Ventilationstest - In-Situ-Verfahren zur Permeabilitätsbestimmung im Kristallin, Nagra Technical Report NTB 91-02, Wettingen, Switzerland, 1991.

Levenberg, K., A method for the solution of certain nonlinear problems in least squares, *Quart. Appl. Math.*, 2, 164-168, 1944.

Luckner, L., M. T. van Genuchten, and D. Nielsen, A consistent set of parametric models for the two-phase flow of immiscible fluids in the subsurface, *Water Resour. Res.*, 25 (10), 2187-2193, 1989.

Marquardt, D. W., An algorithm for least-squares estimation of nonlinear parameters, *J. Soc. Indust. Appl. Math.*, 11(2), 431-441, 1963.

Mualem, Y., A new model for predicting the hydraulic conductivity for unsaturated porous media, *Water Resour. Res.*, 12 (3), 513-522, 1976.

Narasimhan, T. N., and P. A. Witherspoon, An integrated finite difference method for analyzing fluid flow in porous media, *Water Resour. Res.*, 12 (9), 57 - 64, 1976.

Neuman, S. P., Calibration of distributed parameter groundwater flow models viewed as a multiple-objective decision process under uncertainty, *Water Resour. Res.*, 9(4), 1006-1021, 1973.

Pruess, K., TOUGH User's Guide, Nuclear Regulatory Commission, Report LBL-20700, Lawrence Berkeley Laboratory, Berkeley, CA, 1987.

Pruess, K., TOUGH2 - A general-purpose numerical simulator for multiphase fluid and heat flow, Report LBL-29400, Lawrence Berkeley Laboratory, Berkeley, CA, 1991.

Pruess, K., and T. N. Narasimhan, A practical method for modeling fluid and heat flow in fractured porous media, *Society of Petroleum Engineers Journal*, 25(1), 14-26, 1985.

Scales, L. E., Introduction to non-linear optimization, Springer, New York, 1985.

Seager, M., A SLAP for the masses, Lawrence Livermore Nat. Laboratory Technical Report, UCRL-100267, 1988.

van Genuchten, M. T., A closed form equation for predicting the hydraulic conductivity of unsaturated soils, *Soil Sci. Soc. Am. J.*, 44(5), 892-898, 1980.

Vargaftik, N. B., Tables on the thermophysical properties of liquids and gases, 2nd ed., John Wiley, NY, 1975.

Vomvoris, S., B. Frieg (eds), Grimsel Test Site, Overview of Nagra field and modeling activities in the Ventilation Drift (1988 - 1990), Nagra Technical Report NTB 91-34, Wettingen, Switzerland, 1991.

Walker, W. R., J. D. Sabey, and D. R. Hampton, Studies of heat transfer and water migration in soils, Department of Agricultural and Chemical Engineering, Colorado State University, Fort Collins, CO, 1981.

Xiang, Y., S. F. Sykes, and N. R. Thomson, A composite L_1 parameter estimator for model fitting in groundwater flow and solute transport simulations, *Water Resour. Res.*, 29(6), 1661-1673, 1993.

Yeh, W. G., Review of parameter estimation procedures in groundwater hydrology: The inverse problem, *Water Resour. Res.*, 22(2), 95-108, 1986.

LAWRENCE BERKELEY LABORATORY
UNIVERSITY OF CALIFORNIA
TECHNICAL INFORMATION DEPARTMENT
BERKELEY, CALIFORNIA 94720